Biogeosciences Discuss., 7, 4987–5009, 2010
www.biogeosciences-discuss.net/7/4987/2010/
doi:10.5194/bgd-7-4987-2010

Biogeosciences Discussions

Oxygenation variability off Northern Chile during the last two centuries

J. A. Díaz-Ochoa[1], S. Pantoja[1], G. J. De Lange[2], C. B. Lange[1], G. E. Sánchez[1], V. R. Acuña[1], P. Muñoz[3], and G. Vargas[4]

[1]Departamento de Oceanografía and Centro de Investigación Oceanográfica en el Pacífico Sur Oriental (FONDAP-COPAS), Universidad de Concepción, Casilla 160-C, Concepción, Chile
[2]Geochemistry Department, Faculty of Geosciences, Utrecht University, Budapestlaan 4, 3584 CD, Utrecht, The Netherlands
[3]Departamento de Biología Marina, Universidad Católica del Norte, Larrondo 1281, Coquimbo, Chile
[4]Departamento de Geología, Universidad de Chile, Casilla 13518 Correo 21, Plaza Ercilla 803, Santiago, Chile

Received: 4 June 2010 – Accepted: 21 June 2010 – Published: 1 July 2010

Correspondence to: J. A. Díaz-Ochoa (jadiaz@udec.cl)

Published by Copernicus Publications on behalf of the European Geosciences Union.

Abstract

The Peru Chile Current ecosystem is characterized by high biological productivity and important fisheries. Although this system is likely to be severely affected by climate change, its response to current global warming is still uncertain. In this paper we analyze 10–166 year old sediments in two cores collected in Mejillones Bay, an anoxic sedimentary setting favorable for preservation of proxies. Based on a 166 year chronology we used indicators of bottom water oxygenation proxies (Mo, V, S, and the (lycopane+n-C_{35})/n-C_{31}) ratio) and surface water productivity (biogenic opal, counts of diatom valves, biogenic Ba, organic carbon and chlorins) to reconstruct environmental variations in Mejillones Bay. We find that at decadal scales, and during the last two centuries, a shift in the coastal marine ecosystem off Northern Chile took place which was characterized by intense ENSO-like activity and large fluctuations in biological export productivity, in bottom water oxygenation, and increased eolic activity (inferred from Ti/Al and Zr/Al). On top of this short-term variability, a gradual increase of sulfidic conditions has occurred being even more intensified since the early 1960s.

1 Introduction

Eastern boundary upwelling systems such as Peru-Chile, California, Canary and Benguela are amongst the richest areas for world fisheries concentrating ~10–20% of world catch in ~0.1% of the ocean (Chavez et al., 2008; Freón et al., 2009). With the exception of the Canary Current these eastern boundary upwelling systems are characterized by the formation of an intense mid-water depth oxygen minimum zone (OMZ) fueled by high levels of organic matter respiration, sluggish circulation and/or the advection of low oxygen waters (Helly and Levin, 2004). The study of such oxygen deficient layers is of particular interest because of their contribution to gas exchanges between the ocean and the atmosphere, including CO_2, at both regional and global scales (Freón et al., 2009). Several studies recently pointed out that during the last

century as climate warmed, anoxia increased in the world ocean (Chan et al., 2008; Diaz and Rosenberg, 2008; Monteiro et al., 2008; Stramma et al., 2008; Keeling et al., 2010 and references therein). In this work we particularly focus on the Peru-Chile Current System's OMZ variability and its relation with biological productivity during the last two centuries.

The relatively shallow (<100–~600 m deep) OMZ off Peru and Chile is strongly affected at interannual timescales by the occurrence of El Niño events during which warm water masses from the Western Equatorial Pacific Ocean intercept with the coastal upwelling zones, oxygenating the shelf and upper slope (Blanco et al., 2002; Arntz et al., 2006; Fuenzalida et al., 2009, and references therein). At longer time scales, enhanced organic carbon burial and higher δ^{15}N have been reported from sediments collected in Northern Chile and Southern Peru between AD 1820 and 1878 (Vargas et al., 2007). This shift has been associated with centennial scale intensification of southerly winds, enhanced upwelling of nutrients to the euphotic zone, and increased primary production as well as with less oxygenation promoting denitrification (Vargas et al., 2004, 2007; Siffedine et al., 2008). In this paper we use information provided by redox-sensitive elements Mo, V and S and the (lycopane+n-C_{35})/n-C_{31} ratio preserved in the sediments as bottom water oxygenation proxies. The signal of paleoxygenation is examined in a multi-proxy framework taking into account biological productivity and the occurrence of historical El Niño Southern Oscillation (ENSO) events. On this basis, we will not only be able to reconstruct the upper sediment and water column redox conditions during the last two centuries, but also to assess underlying mechanisms responsible for oxygenation variations at decadal scales and provide insight on the response of the Peru-Chile upwelling ecosystem to recent climate change.

2 Study area

Mejillones Bay (~23° S– ~70° 25′ W, off the Atacama Desert) is a relatively shallow water body (depth <125 m) in the Peru-Chile Current System (Fig. 1), characterized by

high biological productivity (1070 g C m^{-2} y^{-1}; Marin et al., 1993), restricted water circulation, low turbulence, and low concentrations of dissolved oxygen in bottom waters (Escribano, 1998; Marin et al., 2003; Valdés et al., 2003; Vargas et al., 2004). The high primary productivity of the Mejillones area is sustained by the quasi-permanent upwelling of nutrient-rich Equatorial Subsurface Water off Angamos Point and the formation of filaments (Marin et al., 2001). However, several studies conducted about the 1997–1998 El Niño phenomenon suggested that this general pattern may be altered by the presence of Kelvin poleward waves which increase sea surface temperature and deepen both the thermocline and the oxycline (e.g., González et al., 1998; Iriarte et al., 2000; Fuenzalida et al., 2009).

Presently, sediments in Mejillones Bay are deposited under oxygen-depleted conditions and good preservation of organic matter and biogenic proxies such as diatom valves, tests of foraminifers and fish scales is evidenced by the presence of laminated sediments (e.g., Ortlieb et al., 2000; Valdés et al., 2004; Vargas et al., 2004; Díaz-Ochoa et al., 2008; Vargas et al., 2007; Caniupán et al., 2009). High rates of primary productivity promote high export rates of agglomerated (brown and black) organic matter as well as high rates of sulfate-reduction which favor precipitation of metallic sulfurs from bottom water to sediments (Valdés et al., 2004), as observed in other environments (Zheng et al., 2000). On the other hand, periods of lower primary productivity, organic matter deposition, and sulfate reduction rates are recorded as dispersed and yellowish organic matter (Valdés et al., 2004).

Mejillones Bay provides a privileged setting for paleoceanographic reconstructions and its sedimentary record appears to reflect conditions for the adjacent coastal ecosystem (Vargas et al., 2007).

3 Material and methods

We analyzed two sediment cores collected during the ZOMEI cruise aboard the AGOR Vidal Gormáz of the Chilean Navy, between 25 September and 1 October 2005 in Mejil-

lones Bay. The first core was collected with a box corer at 23° 03.3′ S, 70° 27.4′ W (BC-3; Fig. 1). This core was subsampled on board using four acrylic plates (50×10 cm) and then stored at 2 °C for further analysis in the laboratory. One of the acrylic plates (BC-3C) was subsampled with a resolution of 0.5 cm for dating based on ^{210}Pb activities (Caniupán et al., 2009), whereas another plate (BC-3D) was used for measuring the contents of biogenic opal (SiO_2), organic carbon (C_{org}), and chlorins, as well as for analyzing physical properties (e.g. water content, dry bulk density; data available from Caniupán et al., 2009). Although data for BC-3D were acquired with laminae resolution, here we present the results averaged in 0.5 cm intervals. Plate BC-3D was dated by lateral correlation with plate BC-3C using magnetic susceptibility profiles (Caniupán et al., 2009).

The second core was collected with a multicorer at 23° 2.6′ S, 70° 27.1′ W (MUC-1B; Fig. 1). MUC-1B was sectioned onboard every 0.5 cm and samples were stored in plastic bags at 4 °C. A chronology for MUC-1B was established by measuring ^{210}Pb activities and computing ages with the constant rate of supply model (CRS; Appleby and Oldfield, 1978; Binford, 1990). At core depths where the CRS could not be applied, we used stratigraphic correlations with other dated cores collected in the same location (i.e. $CaCO_3$ content of core F981A collected in 1998, Vargas et al., 2007) or in a nearby location (i.e. several stratigraphic features observed in core BC-3 by Caniupán et al., 2009) to extrapolate ages downcore by simple linear regression. In fact we correlated core MUC-1B with core BC-3D using the presence of a "spongy" layer (see description in Sect. 4.2) and a disturbed layer caused by dredging works of the Mejillones harbor (Grillet et al., 2001; Caniupán et al., 2009). Conducted at the end of 2002, the works of dredging of the Mejillones harbor produced resuspension of sediment in the upper ∼5 cm of BC-3 associated with higher magnetic susceptibility values and possibly high Fe contents (Caniupán et al., 2009). In core MUC-1B sediment resuspension corresponds to strong fluctuations of density and increased accumulation of Al and Fe. Therefore, we infer that the upper 4.5 cm of core MUC-1B correspond to harbor dredging perturbations and hereon assign to it an age of ∼2003. In addition, an

extremely dense layer near the base of MUC-1B was correlated with a maximal density layer probably associated with an earthquake occurred near Cobija, Northern Chile, in AD 1836 (Caniupán et al., 2009). The chronology of ENSO events occurred during the 19th century was taken from Garcia-Herrera et al. (2008) and Gergis and Fowler (2009), and the consistency of the Gergis and Fowler (2009) chronology for the ENSO events until the end of the 20th century was checked with the chronology provided by Trenberth (1997). To facilitate the comparison between ENSO chronologies and our sediment records the total number of El Niño and La Niña were grouped within the same time intervals established with the age model estimated for core MUC-1B.

Sections of core MUC-1B were freeze dried, powdered with an agate mortar and subjected to a mixture of strong acids (72% $HClO_4$, 4.5% HNO_3, and 48% HF) for determining elemental composition (Al, Ba, Fe, Mo, Na, S, Ti, V, Zr) with an inductively coupled plasma optical emission spectrometer (ICP-OES) according to Schenau and De Lange (2000).

For core MUC-1B, we used biogenic opal measured with the method of Mortlock and Froelich (1989) and counts of diatom valves as productivity proxies (Sánchez, 2009) as well as the content of biogenic Ba (bioBa) extracted with 2M NH_4Cl (pH=7) following the method of Rutten and De Lange (2002) for several intervals in the core. We also computed biogenic Ba using the normative method (Ba_{bio}) including total Ba and detrital Ba/Al ($(Ba/Al)_{det}$) estimated as the difference between total Ba (Ba_{tot}) and bioBa and using the equation $Ba_{bio}=Ba_{tot}-(Al\times(Ba/Al)_{det})$ (Reitz et al., 2004). With a resolution of 0.5 cm, Ba_{bio} calculation took into account the interval between minimal and maximal $(Ba/Al)_{det}$ observed in MUC-1B and provided a reference framework for interpreting lower resolution (∼1 cm) direct measurements of bioBa.

Most elements measured by ICP-OES were normalized with Al to correct for variable carbonate content. Percent deviations from the mean were computed for Ti/Al and Zr/Al and their summation was used as a proxy for terrigenous material input. Mo/Al and V/Al were interpreted as paleoredox proxies whereas S, corrected for seawater salt content, was used as a proxy of sulfate reduction intensity (Nameroff et al., 2004; Böning et al.,

2005).

In addition, we studied the depth variation of the ratio (lycopane+n-C_{35})/n-C_{31} as an organic paleoredox proxy since preservation of lycopane is enhanced under anoxic conditions (e.g., Sinninghe Damsté et al., 2003). Lycopane was extracted from ∼0.6 g sediment samples of MUC-1B and analyzed using an Agilent Technologies 6890 instrument equipped with an Agilent Technologies 5973 mass spectrometer. The chromatograph was equipped with a fused silica capillary column (30 m length, i.d.=0.25 mm HP5-MS, film thickness=0.25 µm) and an automated injection system. Helium was used as the carrier gas (101.9 kPa pressure) with a flow of 24.4 mL/min, the oven was programmed from 80 °C to 130 °C at a rate of 20 °C/min, and then to 310 °C (32.5 min) at a rate of 4 °C/min. The mass spectrometer was programmed to 70 eV and compounds were identified based on the relative retention time and by comparison with mass spectra reported in literature (Kimble et al., 1974; Volkman, 2005).

4 Results

4.1 Chronology

A comparison of several proxy data in cores MUC-1B, F981-A and BC-3 is presented in Fig. 2. In core MUC-1B high and relatively uniform values of ^{210}Pb, Fe/Al and %$CaCO_3$ are apparent within the top 4.5 cm whereas Fe/Al and %$CaCO_3$ display local minima within the spongy layer (see Sect. 4.2) between 20 and 21.5 cm core depth (Fig. 2a,b). The layer affected by the Mejillones harbor dredging works during late 2002 as inferred by increased magnetic susceptibility and rather uniform ^{210}Pb activities in core BC-3 is also shown (Fig. 2d). In addition, we present the correlation between several %$CaCO_3$ peaks in cores MUC-1B and F98-1A (Fig. 2b,c) as well as the correlation established by the presence of a spongy layer in cores MUC-1B and BC-3 (Fig. 2a,b,d,e). The final integrated age model for core MUC-1B, resulted from the combination of the CRS model fitted to ^{210}Pb excess in the upper 10 cm (the interval between 10 and 15 cm

showed anomalous ^{210}Pb distributions that violated the steady state assumption) and stratigraphic correlations with cores F98-1A and BC-3 extrapolated deeper downcore (Fig. 2f,g).

A series of ENSO events based on the recent chronology proposed by Gergis and Fowler (2009) and the list of events since 1950 by Trenberth (1997) is presented in Table 2. In these data are remarkable several periods with maximal frequency of El Niño (i.e. four events in 1975–1980, 1937–1941, 1902–1906, and 1845–1850) and La Niña events (i.e. four or more events in 1906–1911, 1893–1898, and 1871–1876).

4.2 Sediment characteristics

Coloration of both BC-3 and MUC-1B was mostly olive green-gray (Munsell chart scale 7.5Y 3/2) and exhibited a succession of dark and light laminations. Both cores showed the presence of a spongy layer (green rectangles in Fig. 2a,b,d), which was considerably bright (Munsell scale 7.5Y 4/4; e.g. the band between AD 1861 and 1870 of core BC-3 in Fig. 2e), with high water content (MUC-1B: >90% w/w) and low density (MUC-1B: <0.1 g cm^{-3}). The sediments in cores MUC-1B and BC-3 were also rich in biogenic opal (MUC-1B: ∼17–>50%-SiO_2 vs. BC-3: ∼19–55%-SiO_2; Fig. 3a) and diatom valves (MUC-1B: $<1\times10^8$ and $>10\times10^8$ valves g^{-1} ; Fig. 3b), Ba_{bio} (MUC-1B: 90–355 ppm; Fig. 3c), chlorins (MUC-1B: 197–735 mmol g^{-1}; Fig. 3d), C_{org} (BC-3: 1–9%; Fig. 3e), and fish debris (MUC-1B: Díaz-Ochoa et al., 2008).

4.3 Paleoproductivity proxies

The biogenic opal record displayed a decreasing long-term trend with high values (%SiO_2∼>50% w/w in core BC-3D) during the early 1800s and lower and more variable values (%SiO_2∼<35% in both cores MUC-1B and BC-3D) throughout the rest of the 19th century. However, since the mid 20th century biogenic opal in both cores recovered and frequently attained values >40% (Fig. 3a). In contrast with long-term trends at shorter time scales biogenic opal records in MUC-1B and BC-3D seem mostly to

counter-act with the exception of a brief interval during the early 1870s and during the 1950s, the latter coincident with anomalies of ^{210}Pb (Fig. 3a,d). Within the spongy layer (~the 1860s) biogenic opal was quite variable and by the early 1870s the previous decreasing trend disappeared (Fig. 3a). In addition, since 1863, and throughout the rest of the 1860s, diatom valves declined abruptly from $\sim 10\times10^8$ g^{-1} to $\sim<2\times10^8$ g^{-1} while the contribution of valves of warm-water species (especially those of *Rhizosolenia formosa* Peragallo) increased by a factor of 3 (Table 1). Coincident, there is a strong decline in C_{org} content (BC-3D). This minimum may also be reflected in Ba_{bio} (MUC-1B) and chlorins (BC-3D) but is not observed in biogenic opal (Fig. 3).

Biogenic Ba directly determined from selective extractions (bioBa) oscillated at 210±77 ppm in core MUC-1B (Fig. 3c) whereas more detailed Ba_{bio}, determined from total Ba and the detrital Ba/Al (see Material and Methods section), permitted to describe a general trend for biogenic Ba (the thin lines of Fig. 3c). Moreover, bioBa showed some coherency with biogenic opal content (r=0.57, p<0.01) and diatom valves count (r=0.67, p<0.01) in core MUC-1B (Fig. 3c), but not with S (r=−0.30, p>0.1) nor Mo/Al (r=0.15, p>0.4). Furthermore, for core BC-3D it is remarkable that the productivity proxy chlorins does not correlate with biogenic opal (r=−0.0002, p<0.998) whereas C_{org} is negatively correlated with biogenic opal (r=−0.61, p<0.0001) (Fig. 3). Accordingly, the general depth distribution of biogenic Ba is consistent with that of chlorins and C_{org}, but all of these do not show a clear relationship with biogenic opal and diatom valve counts.

4.4 Paleoxygenation proxies

Depth distribution patterns for redox-sensitive element ratios Mo/Al and V/Al are similar and display high and coherent variability (r=0.83, p<0.001; Fig. 4). These patterns are roughly replicated by the (lycopane+n-C_{35})/n-C_{31} ratio during several periods (Fig. 4a,b). All the redox-sensitive proxies display a general trend towards higher values to the present, a trend which appears more pronounced for S and Fe/Al proxies which in addition are strongly correlated with the summation of percent deviation from

the mean of terrigenous proxies Ti/Al and Zr/Al (r=0.86, p<0.0001) (Fig. 4c,d).

5 Discussion

Two sediment cores have been collected in Mejillones Bay in Northern Chile, the only setting of the Chilean margin where laminated sediments have been reported (e.g., Ortlieb et al., 2000; Vargas et al., 2004). Using bottom-water oxygenation proxies Mo/Al, V/Al and S, and the ratio (lycopane+n-C_{35})/n-C_{31} we have investigated changes in oxygenation conditions between ~1836 and ~2002.

Cores MUC-1B and BC-3 were successfully correlated and a constrained age model could be obtained for core MUC-1B in order to study the signals of oxygenation and productivity observed during the last two centuries in Mejillones bay. However, because coastal upwelling areas such as the Peru-Chile Current are simultaneously characterized by high biological productivity and the formation of an Oxygen Minimum Zone, proxies' interpretation is not always straight forward. Consequently, we focus on the interpretation of paleoproductivity proxies as a function of bottom water oxygenation and their related preservation.

5.1 Oxygenation and productivity proxies

Redox-sensitive trace metals in core MUC-1B are much enriched, especially since the mid 1850s, suggesting more oxygenated conditions in the bottom water before that time. These observations are consistent with previous findings pointing to a transition period between 1820 and 1878 characterized by stronger upwelling favorable coastal winds off Northern Chile and Peru (Vargas et al., 2007; Fig. 4).

In addition, the spongy layer corresponding to the 1860s seems coincident with a time interval when very strong ENSO events occurred in the Pacific basin (i.e. La Niña years: 1860, 1861, and 1863: Gergis and Fowler, 2009; El Niño years: 1866 and 1868; Garcia-Herrera et al., 2008). As a whole, the spongy layer appears mostly

dominated by La Niña like conditions during the early 1860s and concomitantly higher biological productivity (i.e. higher biogenic Ba, chlorins and C_{org} contents) and stronger low oxygen conditions (i.e. higher Mo/Al, V/Al and (lycopane+*n*-C_{35})/*n*-C_{31}) in the bottom water. In contrast, towards the late 1860s a simultaneous drop in biogenic Ba, chlorins and C_{org} and lower Mo/Al, V/Al and (lycopane+*n*-C_{35})/*n*-C_{31}) as well as minimal S were observed (Figs. 3a and 4a,b). Moreover, the upper boundary of the spongy layer that includes the interval between 1867 and 1869, reported as a period with extended El Niño events (Garcia-Herrera et al., 2008), is characterized by a high abundance of the warm water diatom species *R. formosa* in the sediments (Table 1).

Oxygenation proxies Mo/Al and V/Al in core MUC-1B approximately describe a series of peaks and troughs which, to some extent, could be related with ENSO events documented for periods such as the early 1900s or between the 1930s and the early 1940s characterized by a notable reduction in the number of La Niña events (Gergis and Fowler, 2009; Table 2). Moreover, Mo/Al and V/Al variability is correlated positively with biogenic opal fluctuations in core MUC-1B. However, as shown for the spongy layer, the relationship between oxygenation/productivity and ENSO activity is obscured by an averaging effect produced by the inclusion of several events within the same sampling interval. Thus, the only way to separate unequivocally the signals associated with particular events would be an analysis at laminae resolution. On the other hand, it seems highly probable that the cycles described by the redox proxies Mo/Al, V/Al and (lycopane+*n*-C_{35})/*n*-C_{31} would be associated with ENSO-like variability accompanied by biological productivity and oxygenation fluctuations in Mejillones bay.

Productivity proxies biogenic Ba, chlorins and C_{org} display a coherent oscillating pattern (Fig. 3c–e) that roughly resembles to decadal cycles such as those proposed by Vargas et al. (2007). According to our data, such pattern is characterized by periods of sustained increase of primary production (e.g. the ~80 years period of growing productivity between the late 1830s and the early 1920s or the period since the early 1950s) followed by periods with rapid declines like those observed between the 1920s and the late 1940s (Fig. 3c–e). Taking into account that Mejillones bay is a highly pro-

ductive coastal upwelling ecosystem where diatoms are the dominant phytoplankton, it is surprising that biogenic opal signals in cores MUC-1B and BC-3 seem to counteract (Fig. 3a). We speculate that in the study area there might be shifts in diatom blooms depending on the distance from the coast and/or depth or, alternatively, that this counter-acting pattern could be the result of wave action at different depths.

5.1.1 Preservation issues

The close relationship between sulfur content and the Fe/Al ratio (Fig. 4c) strongly suggests that most of the reduced sulfur deposited in the sediment is incorporated into metallic sulfides such as pyrite. It is also supported by the general pattern of biogenic Ba that corresponds to those for chlorins and C_{org} and is not anti-correlated with that of S. Therefore, we suggest that the sedimentary environment in Mejillones bay has become more sulfidic since the mid 19th century and that by the early 1960s it experienced a rapid shift to even more sulfidic conditions (Fig. 4c). This is not only expressed as a long term increase of sulfidic conditions, but also, as a decadal oscillation of enhanced primary and export production that is probably associated to ENSO-like frequency and increased intensity of upwelling favorable winds off Northern Chile (Vargas et al., 2007).

In addition, it has been suggested that organic carbon preservation depends on the redox conditions in surface sediments and successive oxygenation oscillations would have the net effect of reducing preservation of chlorophyll and degradation products (Sun et al., 2002). In this sense, the increased frequency of ENSO events documented since the second half of the 20th century (e.g., Trenberth, 1997) might have produced a combined productivity-preservation signal in the sedimentary record of the Mejillones bay. It is interesting to note that only S and chlorins have a generally increasing trend towards the present (i.e. since the 1960s) whereas such trend is not observed for C_{org} suggesting increased preservation of chlorins under stronger sulfidic conditions supported by the evidence of less efficient degradation of chlorophyll in anoxic than oxic sediments (Sun et al., 1993). Based on the latter interpretation, the productivity and

bottom-water oxygenation proxies analyzed in this work provide evidence to confirm the hypothesis proposed by Vargas et al. (2007) that the marine coastal ecosystem off Northern Chile has experienced a shift since the mid 19th century towards increased biological productivity due to stronger upwelling favorable winds (i.e. increased input of Ti and Zr, Fig. 4d). Moreover, the record of proxies presented indicates that the Mejillones bay have experienced a new and abrupt shift since the early 1960s that is pushing the ecosystem to even more productive and more sulfidic conditions than those produced since the shift occurred between 1820 and 1878.

6 Conclusions

The sediment of Mejillones bay have recorded during the last two centuries what seems to correspond to a shift in the coastal marine ecosystem off Northern Chile characterized by intense ENSO-like activity and large fluctuations of both biological export productivity and bottom water oxygenation. In addition, in the long term, such variability has resulted in a constant increase of sulfidic conditions in the environment, pointing to more sustained oxygen-depleted or even sulfidic (sedimentary) environmental conditions. The latter conditions appear to have intensified since the early 1960s, which may provide insight on the response of the Peru-Chile upwelling ecosystem to recent climate change.

Acknowledgements. This research was funded by FONDECYT grant 3090040, FONDECYT grant 1040503 and the Center for Oceanographic Research in the Eastern South Pacific (COPAS), Universidad de Concepción. JADO acknowledges the support of POGO and the agreement Fundación Andes/Wood Hole Oceanographic Institution/University of Concepción for funding two research visits to the Marine Geochemistry Laboratory, Geosciences, Utrecht University.

References

Appleby, P. and Olfield, F.: The calculation of lead-210 dates assuming a constant rate of supply of unsupported ^{210}Pb to the sediment, Catena, 1–8, 1978.

Arntz, W. E., Gallardo, V. A., Gutiérrez, D., Isla, E., Levin, L. A., Mendo, J., Neira, C., Rowe, G. T., Tarazona, J., and Wolff, M.: El Niño and similar perturbation effects on the benthos of the Humboldt, California, and Benguela Current upwelling ecosystems, Adv. Geosci., 6, 243–265, doi:10.5194/adgeo-6-243-2006, 2006.

Binford, M.: Calculation and uncertainty analysis of ^{210}Pb date for PIRLA project lake sediment cores, Journal of Paleolimnology, 3, 253–267, 1990

Blanco, J., Carr, M-E., Thomas, A., and Strub, T.: Hydrographic conditions off Northern Chile during the 1996–1997 La Niña and El Niño events, J. Geophys. Res., 107, C3, doi:10.1029/2001JC001002, 2002.

Böning, P., Cuypers, S., Grunwald, M., Schnetger, B., and Brumsack, H-J.: Geochemical characteristics of Chilean upwelling sediments at ∼36° S, Mar. Geol., 220, 1–21, 2005.

Caniupán, M., Villaseñor, T., Pantoja, S., Lange, C. B., Vargas, G., Muñoz, P., and Salamanca, M.: Sedimentos laminados de la Bahí a Mejillones como registro de cambios temporales en la productividad fitoplanctónica de los últimos ∼200 años, Rev. Chil. Hist. Nat., 82, 83–96, 2009.

Chan, F., Barth, J., Lubchenco, J., Kirincich, A., Weeks, H., Peterson, W., and Menge, B.: Emergence of anoxia in the California Current Large Marine Ecosystem, Science, 319, 920, doi:10.1126/science.1149016, 2008.

Chavez, F., Bertrand, A., Guevara-Carrasco, R., Soler, P., and Csirke, J.: The Northern Humboldt Current System: brief history, present status and a view towards the future, Prog. Oceanogr., 79, 95–105, 2008.

Diaz, R. and Rosenberg, R.: Spreading dead zones and consequences for marine ecosystems, Science, 231, 926–929, 2008.

Díaz-Ochoa, J. A., Lange, C. B., and De Lange, G. J.: Preservación y abundancia de escamas de peces en sedimentos del margen continental de Chile (21–36° S), Rev. Chil. Hist. Nat., 81, 561–574, 2008.

Escribano, R.: Population dynamics of *Calanus chilensis* in Chilean eastern boundary Humboldt Current, Fish. Oceanogr., 7, 245–251, 1998.

Freon, P., Barange, M., and Aristegui, J.: Eastern boundary upwelling ecosystems: integrative

and comparative approaches, Prog. Oceanogr., 83, 1–14, 2009.
Fuenzalida, R., Schneider, W., Garcés-Vargas, J., Bravo, L., and Lange, C.: Vertical and horizontal extension of the oxygen minimum zone in the Eastern South Pacific Ocean, Deep-Sea Res. Pt. II, 56, 992–1003, 2009.
Garcia-Herrera, R., Diaz, H. F., Garcia, R. R., Prieto, M. R., Barriopedro, D., Moyano, R., and Hernandez, E.: A chronology of El Niño events from primary documentary sources in Northern Peru, J. Climate, 21, 1948–1962, doi:10.1175/2007JCLI1830.1, 2008.
Gergis, J. and Fowler, A.: A history of ENSO events since A. D. 1525: implications for future climate change, Climatic Change, 92, 343–387, 2009.
González, H., Daneri, G., Figueroa, D., Iriarte, J., Lefevre, N., Pizarro, G., Quiñones, R., Sobrazo, M., and Troncoso, A.: Producción primaria y su destino en la trama trófica pelágica y océano profundo e intercambio océano-atmósfera de CO_2 en la zona norte de la corriente de Humboldt (23° S): posibles efectos del evento El Niño, 1997–98 en Chile, Rev. Chil. Hist. Nat., 71, 429–458, 1998.
Grillet, L., Ratliff, M., Montgomery, R., Monter, E.: Chile Mejillones Port Project (CH-0162): environmental and social impact report (ESIR), Inter-American Development Bank, 50 pp., http://www.iadb.org/pri/projDocs/CH0162_R_E.pdf, last access: 15 December 2009, 2001.
Helly, J. and Levin, L.: Global distribution of naturally occurring marine hypoxia on continental margins, Deep-Sea Res. Pt. I, 51, 1159–1168, 2004.
Iriarte, J., Pizarro, G., Troncoso, V., and Sobarzo, M.: Primary production and biomass size-fractioned phytoplankton off Antofagasta, Chile (23–24° S) during pre-El Niño and El Niño 1997, J. Marine Syst., 26, 37–51, 2000.
Keeling, R., Körtzinger, A., and Gruber, N.: Ocean deoxygenation in a warming world, Annu. Rev. Mar. Sci., 2, 199–229, 2010.
Kimble, B., Maxwell, J., Philp, R., Eglinton, G., Albrecht, P., Ensminger, A., Arpino, P., and Ourisson, G.: Tri- and tetraterpenoid hydrocarbons in the Messel oil shale, Geochim. Cosmochim. Ac., 38, 1165–1181, 1974.
Marín, V., Escribano, R., Delgado, L. E., Olivares, G., and Hidalgo, P.: Nearshore circulation in a coastal upwelling site off the Northern Humboldt Current System, Cont. Shelf Res., 21, 1317–1329, 2001.
Marín, V., Delgado, L., and Escribano, R.: Upwelling shadows at Mejillones Bay (Northern Chilean coast): remote sensing in situ analysis, Invest. Marinas, Valparaíso, 31, 47–55, 2003.

Marín, V., Rodríguez, L., Vallejo, L., Fuenteseca, J., and Oyarce, E.: Dinámica primaveral de la productividad primaria de Bahí a Mejillones del Sur (Antofagasta, Chile), Rev. Chil. Hist. Nat., 66, 479–491, 1993.
Monteiro, P., Plas, A., Mélice, J.-L., and Florenchie, P.: Interannual hypoxia variability in a coastal upwelling system: ocean-shelf exchange, climate ecosystem-state implications, Deep-Sea Res. Pt. I, 55, 436–450, 2008.
Mortlock, R. and Froelich, P.: A simple method for rapid determination of biogenic opal in pelagic marine sediments, Deep-Sea Research, 36, 1415–1426, 1989.
Nameroff, T., Calvert, S., and Murray, J: Glacial-interglacial variability in the Eastern Tropical North Pacific oxygen minimum zone recorded by redox-sensitive trace metals, Paleoceanography, 19, PA1010, doi:10.1029/2003PA000912, 2004.
Ortlieb, L., Escribano, R., Follegati, R., Zúñiga, O., Kong, I., Rodríguez, L., Valdés, J., Guzman, N., and Iratchet, P.: Recording of ocean-climate changes during the last 2000 years in a hypoxic marine environment off Northern Chile (23° S), Rev. Chil. Hist. Nat., 73, 221–242, 2000.
Reitz, A., Pfeifer, K., De Lange, G. J., and Klump, J.: Biogenic barium and the detritial Ba/Al ratio: a comparison of their direct and indirect determination, Mar. Geol., 204, 289–300, 2004.
Rutten, A. and De Lange, G. J.: A novel selective extraction of barite, and its application to eastern Mediterranean sediments, Earth Planet. Sc. Lett., 198, 11–24, 2002.
Sánchez, G. E.: Variabilidad de la producción silícea durante los últimos doscientos años, basada en diatomeas planctónicas y sílice biogénico en sedimentos del margen continental de Chile, Ph.D. thesis, Universidad de Concepción, Concepción (Chile), 211 pp., 2009.
Schenau, S. and De Lange, G. J.: A novel chemical method to quantify fish debris in marine sediments, Limnol. Oceanogr., 45, 963–971, 2000.
Siffedine, A., Gutiérrez, D., Ortlieb, L., Boucher, H., Velazco, F., Field, D., Vargas, G., Boussafir, M., Salvatecci, R., Ferreira, V., García, M., Valdés, J., Caquineau, S., Mandeng Yogo, M., Cetin, F., Solis, J., Soler, P., and Baumgartner, T.: Laminated sediments from the Peruvian continental slope: a 500 year record of upwelling system productivity, terrestrial runoff and redox conditions, Prog. Oceanogr., 79, 190–197, 2008.
Sinninghe Damsté, J., Kuypers, M., Schouten, S., Schulte, S., and Rullkötter, J.: The lycopane/C_{31} n-alkane ratio as a proxy to assess palaeoxicity during sediment deposition, Earth Planet. Sc. Lett., 209, 215–226, 2003.

Stramma, L., Jhonson, G., Sprintall, J., and Mohrholz, V.: Expanding oxygen-minimum zones in the tropical oceans, Science, 320, 655–658, 2008.
Sun, M., Aller, R., Lee, C., and Wakeham, S.: Effects of oxygen and redox oscillation on degradation of cell-associated lipids in superficial marine sediments, Geochim. Cosmochim. Ac., 66, 2003–2012, 2002.
Sun, M., Lee, C., and Aller, R.: Laboratory studies of oxic and anoxic degradation of chlorophyll-*a* in Long Island Sound sediment, Geochim. Cosmochim. Ac., 57, 147–157, 1993.
Trenberth, K. E.: The definition of El Niño, B. Am. Meteorol. Soc., 78, 2771–2777, 1997.
Valdés, J., Ortlieb, L., and Sifeddine, A.: Variaciones del sistema de surgencia de Punta Angamos (23° S) y la zona de mínimo oxígeno durante el pasado reciente. Una aproximación desde el registro sedimentario de la Bahía Mejillones del Sur, Rev. Chil. Hist. Nat., 76, 347–362, 2003.
Valdés, J., Sifeddine, A., Lallier-Verges, E., and Ortlieb, L.: Petrographic and geochemical study of organic matter in surficial laminated sediments from an upwelling system (Mejillones del Sur Bay, Northern Chile), Org. Geochem., 35, 881–894, 2004.
Vargas, G., Ortlieb, L., Pichon, J. J., Bertaux, J., and Pujos, M.: Sedimentary facies and high resolution primary production inferences from laminated diatomaceous sediments off Northern Chile (23° S), Mar. Geol., 211, 79–99, 2004.
Vargas, G., Pantoja, S., Rutllant, J., Lange, C. B., and Ortlieb, L.: Enhancement of coastal upwelling and interdecadal ENSO-like variability in the Peru-Chile Current since the late 19th century, Geophys. Res. Lett., 34, L13607, doi:10.1029/2006GL028812, 2007.
Volkman, J.: Lipid markers for marine organic matter, Hdb. Env. Chem., 2, 27–70, 2005.
Zheng, Y., Anderson, R., van Geen, A., and Kuwabara, J.: Authigenic molybdenum formation in marine sediments: a link to pore water sulfide in the Santa Barbara Basin, Geochim. Cosmochim. Ac., 64, 4165–4178, 2000.

Table 1. Diatom counts in selected core depths around the spongy layer for core MUC-1B collected in Mejillones Bay (Northern Chile). Species are grouped depending of the habitat and/or distribution and expressed as relative abundance (%) (Sánchez, 2009).

Diatom habitat	Depth in core (cm)/ (age)			
	19.5–20 (1876–1871)	20.0–20.5 (1871–1867)	20.5–21 (1867–1863)	21–21.5 (1863–1858)
Warm-temperate	14.91	18.89	43.46	18.25
Upwelling	77.05	70.46	53.95	82.80
Freshwater	0.28	0.30	0.50	0.10
Non-planktonic	0.52	0.52	0.57	0.13
Coastal planktonic	6.30	9.59	1.42	1.67
Tycoplankton	0.95	0.25	0.07	0.06
Total diatoms (valves g^{-1})	4.76×10^8	4.32×10^8	2.06×10^8	10.4×10^8

Table 2. Number of El Niño (EN) and La Niña (LN) events (years) included in the sampling intervals of core MUC-1B (events before 1950 from Gergis and Fowler, 2009 and after that year from Trenberth, 1997).

Period	EN	LN	Period	EN	LN	Period	EN	LN	Period	EN	LN
1997–2003	2	3	1954–1956	0	2	1906–1911	3	4	1858–1863	1	3
1994–1997	2	2	1950–1954	3	2	1902–1906	4	1	1854–1858	3	1
1990–1994	3	0	1946–1950	2	1	1898–1902	3	0	1850–1854	2	2
1986–1990	2	2	1941–1946	3	2	1893–1898	2	4	1845–1850	4	3
1980–1986	3	2	1937–1941	4	0	1889–1893	2	2	1841–1845	1	2
1975–1980	4	2	1933–1937	2	1	1884–1889	3	2	1837–1841	2	1
1971–1975	1	3	1928–1933	2	1	1880–1884	1	1			
1967–1971	3	1	1924–1928	3	0	1876–1880	3	2			
1964–1967	3	2	1919–1924	2	3	1871–1876	1	5			
1962–1964	1	0	1915–1919	2	3	1867–1871	1	3			
1956–1962	2	1	1911–1915	2	0	1863–1867	3	3			

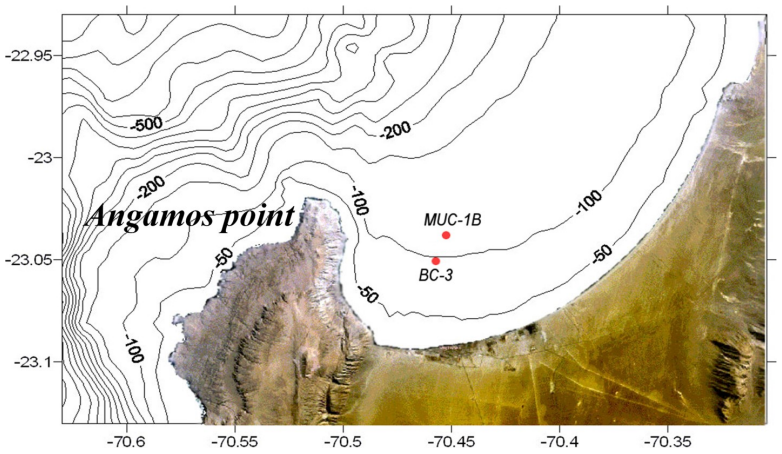

Fig. 1. Study area in Mejillones Bay and sampling locations for cores MUC-1B and BC-3.

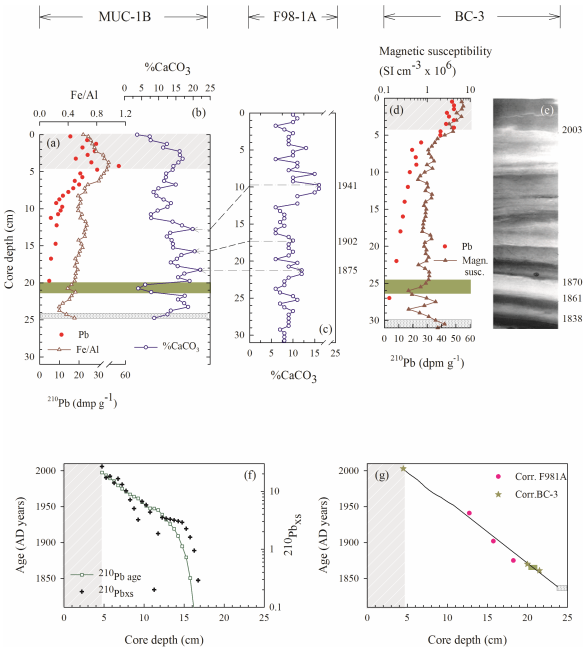

Fig. 2. Fe/Al and ^{210}Pb activity for core MUC-1B **(a)**, calcium carbonate content (%$CaCO_3$) for core MUC-1B **(b)** and core F98-1A **(c)**, magnetic susceptibility and ^{210}Pb activity for core BC-3C **(d)**, contact print of core BC-3D **(e)**, age model estimated from ^{210}Pb excess ($^{210}Pb_{xs}$) with the constant rate of supply model for core MUC-1B **(f)**, and final integrated age model for core MUC-1B including the upper 10 cm ^{210}Pb activities and stratigraphic correlation with cores BC-3 and F98-1A **(g)**. Green areas in (a), (b), (d) and (g) correspond to the "spongy layer" whereas cross-hatched area in the same figures represents harbor construction work starting December 2002, and shaded grey area in (d) represents the 1836 earthquake. Ages in (c) and (e) were obtained from the original age models for core F98-1A (Vargas et al. 2007) and core BC-3D (Caniupán et al., 2009), respectively.

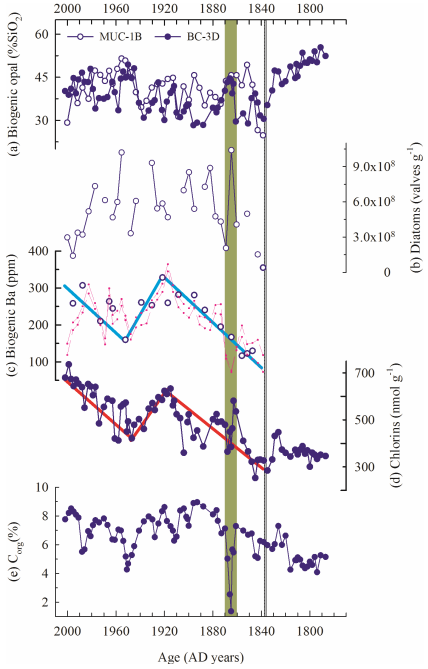

Fig. 3. Productivity proxies biogenic opal (SiO_2) for cores MUC-1B and BC-3D **(a)**, total diatom counts (MUC-1B) **(b)**, biogenic Ba (MUC-1B) **(c)**: (thin pink dashed lines correspond to upper and lower limits of biogenic barium computed from constant detrital Ba/Al of 0.001 and 0.003 (Ba_{bio}) corresponding to the range of direct extractions (bioBa) (open circles)), organic carbon (C_{org}, BC-3D) **(e)**, and chlorins (BC-3D) **(f)**. Common trends between biogenic Ba and chlorins are highlighted with blue and red lines, respectively. Green and shaded grey areas as in Fig. 2.

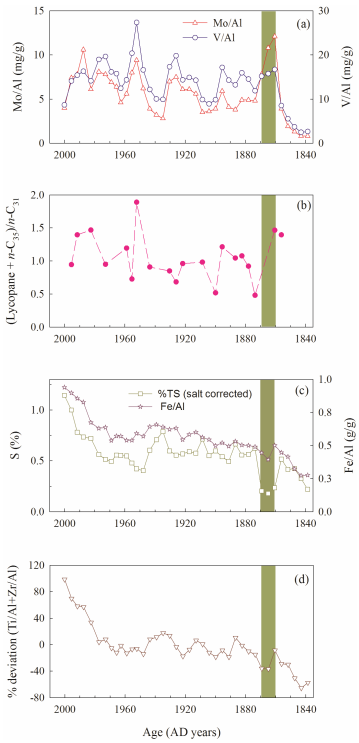

Fig. 4. Normalized bottom-water oxygenation proxies Mo/Al and V/Al **(a)**, (lycopane+n-C_{35})/n-C_{31} ratio **(b)**, percent sulfur (salt corrected) and Fe/Al ratio **(c)**, and summation of percent deviation from the mean of terrigenous proxies Ti/Al and Zr/Al **(d)**. Open symbols for core MUC-1B and closed symbols for core BC-3D. Green area as in Fig. 2.